

Counteranion-Controlled Properties of Polyelectrolyte Multilayers

Mikko Salomäki,^{*,†,§} Taina Laiho,[‡] and Jouko Kankare[†]

Department of Chemistry, University of Turku, FIN-20014 Turku, Finland; Graduate School of Chemical Sensors and Microanalytical Systems (CHEMSEM), Turku, Finland; and Laboratory of Materials Science, University of Turku, FIN-20014 Turku, Finland

Received June 29, 2004; Revised Manuscript Received September 24, 2004

ABSTRACT: Polyelectrolyte multilayers consisting of poly(diallyldimethylammonium chloride) (PDADMA) and poly(sodium 4-styrenesulfonate) (PSS) were studied on a quartz crystal microbalance (QCM) utilizing a novel method to determine the elastic properties of the films. Since the multilayer was found to consist of a hard core and soft outer layer, as can be realized on the basis of the multilayer zone model, the multilayer films were made thick enough to reveal the elastic properties of the bulk material of the film. Several hundreds of layers were deposited using a fully automated multilayer deposition machine. We found out that, in addition to the increase in the bilayer mass, a remarkable increase of stiffness of the polyelectrolyte multilayer was observed while changing the counteranion used in the deposition process. The increase of stiffness was found to be comparable to the glass transition of common polymers. The increase is attributed to the counteranions that take part in polyelectrolyte charge compensation. The correlation of storage shear modulus and mass density to the hydration entropy of the anion could be clearly observed.

Introduction

Thin polyelectrolyte films can be deposited onto a surface of a substrate by exposing it to the solutions of oppositely charged polyelectrolytes in a sequential order.¹ This layer-by-layer (LbL) technique has proven its usefulness in a variety of materials including synthetic polyelectrolytes, biopolymers,² nanoparticles,³ etc. The main advantage of the method is the nanometer scale control over the whole deposition process, providing a possibility to construct precise multilayer architectures. The individually deposited layers in the multilayer system are highly interpenetrated, and therefore the single-layer deposition of flexible polyelectrolyte can be assumed to increase the mass and thickness of the film but not to develop a discrete layer.^{1,4} The thickness of the deposited polyelectrolyte layer depends on the ionic strength of the polyelectrolyte solution⁴ due to the increased polyelectrolyte charge screening by the counterions. Also, the salt type is an important,⁵ but often neglected, factor affecting the growth process.⁶ The extent of charge screening has been found to vary according to the counterion, following the trend of the Hofmeister series.⁷ However, the multilayer thickness is not the only parameter affected by the increased charge screening. In this study we focus on the effect of counteranion on the elastic properties of the multilayer film.

The elastic properties of the polyelectrolyte multilayers are an interesting area of research. The investigation of elastic properties provides important information about the material, and the ability to control the elasticity might be needed in the possible applications. In general, it is advantageous to understand how the multilayer behaves when deforming stress is applied. Because of the small amount of material, the conven-

tional methods of determining the properties are unfeasible. The elasticity of the multilayer films is estimated only in a few reports. The studies of elastic properties are divided into two basic approaches: compress and shear stress methods. The elastic properties of multilayer microcapsules are determined from a collapse of the microcapsules in an increased osmotic pressure^{8,9} or by applying a load onto a microcapsule with an AFM related device.^{10,11} The elasticity of the multilayer film on a substrate has also been studied by applying AFM force on the surface of the film¹² and utilizing reflection interference contrast microscopy.¹³ As an example of shear methods, the viscoelastic properties of thin polymer and protein films on a solid surface have been estimated by using a quartz crystal microbalance (QCM) in a mode that records not only the frequency shift but also the energy losses of the crystal oscillation.^{14–18} A new method of estimating the elastic properties of the polyelectrolyte multilayers using QCM was presented in our earlier article.¹⁹

Polyelectrolyte multilayers are usually studied in contact with aqueous solutions. This adds a couple of very important factors that have to be taken into account in estimating the elastic properties of the substrate-bound material. The material on the film/solution and presumably on the substrate/film interface is evidently different from the bulk material. A recent report on the film properties proposes that the film in liquid constitutes of three rather different zones.²⁰ Zone I contains a couple of first layers on the surface of the substrate. Layers in the zone I are most probably thin precursor layers, which act as an adhesion material between the substrate and the bulk material. Zone II forms a bulk of the film, where the polyelectrolyte charge compensation is achieved by means of polyelectrolyte complexes via intrinsic charge compensation. Zone III is in direct contact with the solution, and the charge compensation is achieved mainly by the counterions. As a result, zone III could be strongly swollen in pure water. Zone III can additionally extend far away to the solution by tails or loops of polyelectrolyte chain.

[†] Department of Chemistry, University of Turku.

[‡] Laboratory of Materials Science, University of Turku.

[§] Graduate School of Chemical Sensors and Microanalytical Systems (CHEMSEM).

* Corresponding author; e-mail mikko.salomaki@utu.fi.

The interfaces between the zones are rather diffuse.²⁰ When the first few layers are deposited, the zones I and III are formed. If the number of layers is small, from a couple to approximately 10 layers, the softness of zone III apparently determines the viscoelastic properties of the wet multilayer, as our previous results showed.¹⁶ If the number of layers is increased, the growth in multilayer takes place in the zone II. The growth also eventually sets the zones I and III completely apart. This also reduces the effect of the zone III on the viscoelastic properties of the film.¹⁹

The number of layers needed to investigate the properties of the bulk multilayer seems to be greater than in the majority of films described in the literature. In this study we extend the polyelectrolyte thickness scale from nanometers to micrometers by depositing several hundreds of layers on the surface of the quartz crystal. To accomplish our goal, we employ a fully automated LbL machine to build up multilayers with a sufficient number of layers to determine the viscoelastic properties of the bulk material.

Experimental Section

Materials. Poly(sodium 4-styrenesulfonate) (PSS, 70 kDa, from Aldrich), 2-mercaptoethanesulfonic acid, sodium salt (MESA, from Aldrich), and (3-aminopropyl)triethoxysilane (Fluka) were used as received. Poly(diallyldimethylammonium chloride) (PDADMA, 100–200 kDa, from Aldrich) was dialyzed against electrolyte solutions, in a membrane with a nominal M_w cutoff of 3500 (“SnakeSkin” dialysis tubing, Pierce Biotechnology, Inc.) to exchange the counteranions. The 2% (w/w) water solution of PDADMA (150 mL) was dialyzed twice against 5 L of 0.1 M electrolyte solution containing sodium salt of NO_3^- , Br^- , ClO_3^- , BrO_3^- , HCOO^- , or F^- . Dialysis was carried out in a continuous-flow system for 48 h. After that the polymer was dialyzed against water to remove the excess of electrolyte. The chloride form of PDADMA was purified by dialyzing against water. Polymer content was determined by evaporating a known portion of solution and drying to constant weight by first evaporating the excess of water in a rotary evaporator and then heating to 110 °C for 24 h, which was enough to reach a plateau in mass decrease.

Multilayer Preparation for Quartz Crystal Analysis. The polished quartz crystals with gold plating (10 MHz, International Crystal Manufacturer, Oklahoma, or Lap-Tech, Inc., South Bowmanville, Ontario) were rinsed with water and dried. The crystals were cleaned in oxygen and hydrogen plasma before use.²¹ The MESA primer layer was deposited at the gold surface of the crystal in order to obtain a negative ionic charge on the surface (a droplet of 1 mM water solution of MESA for 1 h on the gold surface of the crystal). After that the crystal was placed in a flow cell.

The multilayer films were made by using an automated multilayer deposition system consisting of a flow cell and a computer-controlled peristaltic pump with a multiposition valve for switching between the coating and the rinsing solutions. The general deposition sequence was following: Sequentially a 1.5 mL portion of 10 mM (referring to monomer concentrations) solution of PDADMA or PSS (in 0.1 M aqueous solution of NaNO_3 , NaBr , NaF , NaCl , NaBrO_3 , NaClO_3 , or HCOONa) was injected in to the cell and allowed to adsorb for 15 min. The crystal was then rinsed for 5 min with 20 mL of corresponding 0.1 M electrolyte solution and allowed to stabilize for 15 min before the measurement. The ionic strength of solution inside the cell was kept constant during the whole deposition and measuring process to ensure that there were no swelling and deswelling processes during the measurement. The solutions were deaerated before use by bubbling helium for 30 min.

The crystal parameters were measured as described in detail in our previous publication¹⁷ using a prototype crystal analyzer with impedance detection.²² The flow cell was placed

in a container in thermostat bath with a steady air flow in order to achieve the accurate thermal stability needed in the quartz crystal measurements. The cell temperature was kept constant during the measurement (25 ± 0.03 °C). The whole deposition and measurement system was controlled by a computer program written with the National Instrument's LabVIEW general instrumentation utility.

XPS Measurements. Two 60-layer PDADMA/PSS multilayers, with PSS as a terminating layer, were deposited on the top of the quartz crystals by an abovementioned method, using NaBr and NaBrO_3 as base electrolytes. After deposition the films were thoroughly rinsed with running water for 15 min and blown dry with air.

The X-ray photoelectron spectra were recorded on a Perkin-Elmer PHI 5400 spectrometer. All XPS data were acquired using unmonochromatized $\text{Mg K}\alpha$ radiation (1253.6 eV). The power of the X-ray source was 200 W. The photoelectrons were collected at 45° takeoff angle with a hemispherical analyzer having the constant pass energy of 89.45 eV. Survey spectra of both samples were recorded, and atomic concentrations based on the spectral intensities were calculated. Argon ion etching (3 kV beam voltage and 25 mA emission current) was used to obtain information on the composition as a function of depth.

Results and Discussion

Evaluation of the Multilayer Parameters. To examine the properties of the bulk multilayer by means of QCM, the number of layers must be increased to a couple hundred, at least at these concentrations.¹⁹ The maximum number of layers is limited by the quartz crystal measurement signal, which gets noisy during the film growth due to the energy loss of the crystal oscillation induced by surface loading. In the case of a rapidly growing multilayer, such as the one deposited in NaBr , the limiting number of the layers is a little over 300. Nevertheless, with NaF deposition, we could easily build a multilayer with up to 500 layers or more, since the mass growth seemed to be only a small fraction of the multilayer deposited in NaBr .

The characterization of the multilayers was carried out by means of local acoustic impedance (LAI),²³ a complex valued parameter calculated from the electrical impedance of the quartz crystal oscillator.¹⁴ The elastic parameters of the film were obtained by using the matrix fitting method described in our earlier article.¹⁹ In this method each slice of five layers is described by a matrix that is a representation of Möbius transformation derived from a solution of Riccati equation.²³ The obtainable parameters from the method are bulk acoustic shear impedance (Z), bilayer mass density (m), and dynamic shear modulus (G) derived from the bulk acoustic impedance and assumed density. The assumption that all the bilayers in the film are identical is included in this method. This assumption includes a generalization that bulk multilayer (zone II) determines the film properties, and the zones I and III do not give a notable contribution to the parameters. For that reason the zone II must be entirely formed, and the growth has to be linear before the multilayer can be analyzed with this method. The data qualified for fitting started usually from the 25th layer, ending to the layer numbers between 200 and 400 depending on the depositing electrolyte. The calculated data are presented in Table 1.

Theoretically, the LAI graph should adopt the form of a spiral converging toward the value of bulk acoustic impedance. The spiral form arises from the acoustic resonance of waves propagating in the film. However,

Table 1. Properties of PSS/PDADMA Multilayers Deposited in 0.1 M Sodium Salt of Varying Anions

anion	bulk acoustic impedance, Z (kRayl) ^a	phase angle of bulk acoustic impedance (deg)	bilayer mass density ($\mu\text{g cm}^{-2}$)	storage shear modulus, G' (MPa) ^b	loss modulus, G'' (MPa) ^b	loss angle, δ (deg)
F ⁻	98.9 ± 0.4	21.3 ± 0.3	0.54 ± 0.07	6.00 ± 0.05	5.52 ± 0.05	42.6 ± 0.6
HCOO ⁻	80 ± 2	8.2 ± 0.3	0.532 ± 0.003	5.1 ± 0.2	1.51 ± 0.05	16.5 ± 0.6
BrO ₃ ⁻	76.6 ± 0.9	22.5 ± 0.8	0.9 ± 0.2	3.5 ± 0.2	3.5 ± 0.2	45 ± 2
Cl ⁻	150 ± 20	30 ± 10	0.98 ± 0.02	8 ± 5	15 ± 5	60 ± 20
ClO ₃ ⁻	325 ± 8	4.0 ± 0.6	2.6 ± 0.2	87 ± 4	12.2 ± 0.6	8 ± 2
NO ₃ ⁻	410 ± 6	10.8 ± 0.2	4.34 ± 0.08	130 ± 4	51 ± 2	21.5 ± 0.4
Br ⁻	410 ± 2	13.4 ± 0.2	5.2 ± 0.4	124.9 ± 0.9	63.3 ± 0.5	26.9 ± 0.3

^a Rayl = kg m⁻² s⁻¹. ^b Based on the density 1200 kg m⁻³.

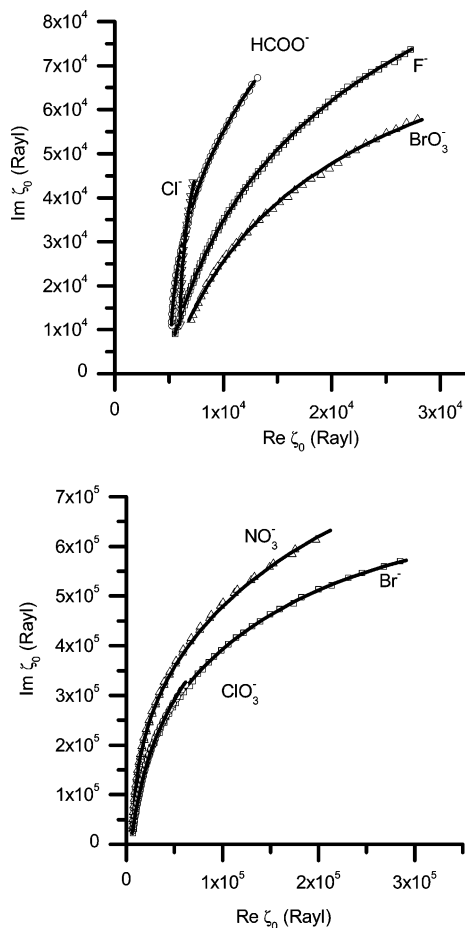


Figure 1. Complex plane representation of local acoustic impedance. Developing multilayers are deposited in 0.1 M sodium salt of corresponding anions. The multilayers have approximately 300–400 layers, except the one deposited in NaCl that has only 130 layers. Curves are obtained by fitting the experimental data.

the end point of the spiral is very far in these measurements because approximately 1000 layers in this concentration scale are needed for one full turn of the spiral.¹⁹ To calculate the parameters of the film, there should at least exist a clear curvature of the spiral in the experimental LAI graph. The LAI graphs (Figure 1) show that the deposited multilayers divide into two separate groups according to their growth rate. The multilayers deposited in NaF, HCOONa, NaBrO₃, and NaCl show a smooth initial growth of complex LAI with a clear curvature in the graph. The multilayers deposited in NaClO₃, NaNO₃, and NaBr exhibit a much higher growth rate and cannot be represented in the same graph. These multilayers have a clear curvature in the complex LAI graph as well. The imaginary part of LAI, which has a direct relation to the mass of the

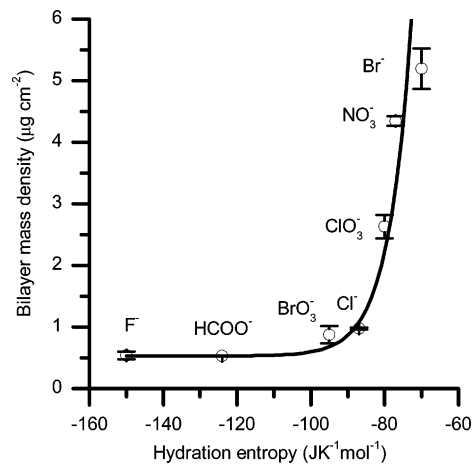


Figure 2. Bilayer mass density of multilayers vs hydration entropy of the counteranion used in the PSS/PDADMA multilayer deposition. The line is added as a guide for the eye.

film,²³ increases with a constant rate during the buildup process. For that reason the growth is most likely linear after the precursor layers are formed in all of the deposited multilayers.

The calculation of the bilayer mass density gave, in addition to the real mass value, also an imaginary part of mass due to the complex nature of the fitting equation.¹⁹ The mass is unquestionably a real valued parameter. The obtained imaginary mass was usually as small as, or somewhat larger than, the experimental error calculated for the real part of mass, varying from 0.5 to 15% of the resulting mass. Therefore, the imaginary mass is considered here as either an experimental error or a slight systematic deviation of the model. The bilayer mass densities obtained from the fitting results are expected to have a correlation with the hydration entropy²⁴ of the counteranion as was already found in our previous article dealing with dry and much thinner multilayers.⁷ The functional form of the correlation in the graph (Figure 2) was found to be seemingly exponential with even a wider variation between the counteranions than with the thinner films.⁷ Two distinct groups of behavior can be distinguished in connection with the bilayer mass density. The multilayers deposited in NaF, HCOONa, NaBrO₃, and NaCl have bilayer mass values increasing steadily in this order. After chloride there is a sharp transition in the graph. The multilayers deposited in NaClO₃, NaNO₃, and NaBr seem to rapidly reach bilayer mass values that are even 10 times higher than in the earlier mentioned multilayers.

Another very important parameter obtained from the measurements is bulk acoustic shear impedance, a complex parameter, which can be used in describing the elastic properties of the material. The complex shear

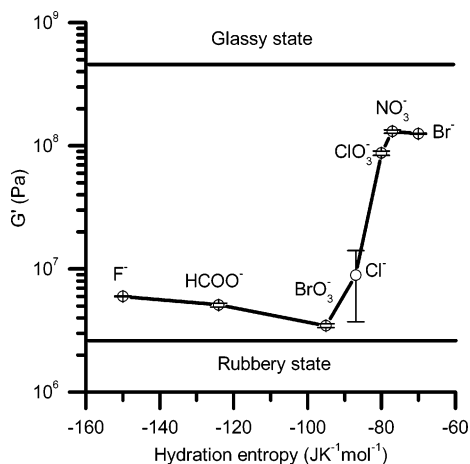


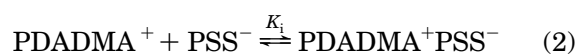
Figure 3. Storage shear modulus of bulk multilayer vs hydration entropy of the counteranion used in the PSS/PDADMA multilayer deposition. The range of shear modulus of the glassy and rubbery state of some common polymers is shown on the graph.²⁸ The comparison between the static shear modulus and the dynamic storage shear modulus can be done if the Voigt viscoelastic model is assumed.

modulus can be derived from the acoustic impedance by assuming the density (ρ) of the material ($Z^2 = \rho G$). At this concept the density of the material is assumed to be near 1200 kg m^{-3} .^{25,26} The complex shear modulus consists of real part G' (storage modulus) and imaginary part G'' (loss modulus). Loss angle is the phase of the complex shear modulus. Its tangent describes the ratio of the energy lost in oscillation (i.e., transformed into heat) between the energy remained in the oscillation. The inverse of shear modulus is shear compliance, denoted by J . The real part of J , often called elastic compliance, can be estimated quite accurately even from thin films.^{16,23,27} However, the determination of loss modulus requires a much thicker film. There is a great variation in the values of loss modulus, even in a film of approximately $5 \mu\text{m}$ thick, depending on the method used in the calculation.¹⁹ This uncertainty is reflected in the loss angle values. It is rather difficult to find an analogous trend between the counteranion and the loss angle as with the mass and storage modulus. However, with one exception (HCOO^-) the loss angle of thin films is higher than the loss angle of thicker films, indicating a more viscous nature of thin films.

The values of storage shear modulus have the same trend as the bilayer mass values (Figure 3.). The breakpoint in the graph is located near the hydration entropy of chloride. The remarkable stiffening of the films follows the increasing hydration entropy of the counteranions. An interesting feature in the graph is that the multilayers deposited in NaF , HCOONa , NaBrO_3 , and NaCl have the storage shear modulus just above the modulus of common polymers in the rubbery state. On the other hand, the shear modulus of the multilayers deposited in NaClO_3 , NaNO_3 , and NaBr are much closer to the values of bulk plastics, i.e., the polymers in their glassy state. The magnitude of the change in stiffness is comparable to the glass transition of a bulk polymer.²⁸ The dramatic increase in the multilayer stiffness is connected to the increased charge screening of the polycation by the counteranions. Such a great increase in stiffness would presumably indicate structural differences between the multilayers deposited in the presence of different electrolytes.

The Function of Counterions. A kind of breakpoint of material properties seems to be located near the hydration entropy value of chloride. It cannot be just a coincidence that it divides the anions into the same groups as in some traditional ion classifications. The existence of two different anion groups can be discussed by using the terms describing the ion–water and ion–macromolecule interactions. The viscosity B coefficient of the Jones–Dole²⁹ empirical expression divides the anions into two main groups. Chaotropic anions (water structure breaking: Br^- , NO_3^- , and ClO_3^-) have negative B coefficients and cosmotropic anions (water structure making: BrO_3^- , HCOO^- , and F^-) have positive B coefficients, while the value of chloride is close to zero in water at $25 \text{ }^\circ\text{C}$.³⁰ The special status of chloride ion is noticed even in the classical Hofmeister series³¹ of anions, where chloride is treated as a median dividing the anions into salting-in and salting-out species. It seems that the chaotropic anions have a special ability to screen the free charges of PDADMA in a very effective manner. As a result, the polyelectrolyte adopts a more dense form and more polyelectrolyte is needed in the surface charge compensation. The counteranions with a higher hydration entropy produce thicker films.⁷ Nevertheless, there is a limit in that correlation because the counteranions having a higher hydration entropy than $-70 \text{ J K}^{-1} \text{ mol}^{-1}$ (the value of bromide) precipitate PDADMA from the solution completely in the used concentration scale.⁷ To this group of ions belong for example ClO_4^- , SCN^- , and I^- . The breakpoint of the PSS/PDADMA multilayer properties was found to be near the hydration entropy of chloride. Despite this, chloride cannot be treated as some universal divider for the multilayer properties. The breakpoint will most likely be dependent on the polyelectrolyte type, ionic strength of counterion, and temperature.

In the deposition process, the charge compensation of strong polyelectrolytes can be achieved via intrinsic and extrinsic charge compensation.³² The charge compensation can be treated as ion-pair formation with pertinent Bjerrum association constants. The ionic association equilibria for extrinsic and intrinsic compensation together with the corresponding association constants K_e and K_i are presented in eqs 1 and 2 in terms of monomer units. The PSS⁻Na⁺ pair is not taken into consideration because in the present study the counteranion was always sodium at a constant concentration. The oppositely charged strong polyelectrolytes favor the intrinsic compensation.³² Therefore, as an assumption, the K_i for strong polyelectrolytes is apparently much higher than the K_e leading to 1:1 polyelectrolyte complexes. The charge screening ability of an ion can be predicted by the hydration entropy of the corresponding ion.⁷ On this basis the polyelectrolyte charge compensation can be adjusted, in addition to ionic strength, by using different counterions. If the counterion has higher hydration entropy, the K_e will be higher inducing a drop in the polymer charge density.



The similarities can be found in weak polyelectrolytes, where the pH-controlled charge density adjusting is a well-known phenomenon.³³ Dramatic changes in multilayer thickness have been observed when the charge

Table 2. XPS Measured Atomic Concentrations at the Surface of the 60-Layer PDADAMA/PSS Multilayer Deposited in 0.1 M Electrolyte

depositing electrolyte	atomic concentrations (%)					
	C	O	S	N	Na	Br
NaBrO ₃	75.26	16.25	4.34	4.15	0	0
NaBr	77.13	13.37	2.95	5.62	0	1.94

density of a polyelectrolyte is lowered modestly.³⁴ By changing the counterion, we have been able to increase the layer thickness in a comparable manner. This provokes a question about the validity of the assumption of 1:1 polyelectrolyte complexes inside the polyelectrolyte multilayer. The presence of counterions has been discussed controversially. Small counterions are claimed to be removed during the washing, leading into locally neutral complex.^{35,36} Despite that it has been shown that the multilayer involves both polyions and small ions,³⁷ up to 30% of the charge sites on polyions could be bound by oppositely charged fluorescent probes.³⁸

X-ray photoelectron spectroscopy is a useful tool for analyzing atom composition near the surface of the substrate. The atomic information can be revealed from the penetration depth of about 2.5 nm. The absence of counterions has been detected with XPS in a polyviologen–PSS system.³⁹ For the XPS measurement we have selected two counteranions containing bromine for the benefit of similarity in the detection. Two 60-layer PDADMA/PSS multilayers were deposited using NaBr and NaBrO₃ as base electrolyte. The counterions represent different classes of ions: BrO₃⁻ is located before the breakpoint in the Figure 3, and Br⁻ is located after the breakpoint in the ion series. Thoroughly water-rinsed films revealed different surface compositions in the XPS spectra. As can be seen in the Table 2, no sodium was detected in either sample. The film deposited in NaBrO₃ demonstrates highly interpenetrated polyelectrolyte multilayer structure with a S/N ratio of ca. 1:1, and no bromine was detected. However, the film deposited in NaBr reveals the presence of counteranions. The charge neutrality was detected on the surface since the amount of positively charged groups was equal to the amount of negatively charged groups, giving a (Br + S)/N ratio of ca. 1:1. About one-third of ammonium groups are considered to be compensated with bromide.

The sequential ion sputtering and XPS provides depth profiling for inorganic samples. Sputtering of organic polymer samples, however, may end up to compositional changes on the surface of the polymer film.⁴⁰ The sputtering of polyelectrolyte multilayer samples brought about changes in atomic composition, namely the disappearance of oxygen which was attributed to the fragmentation of sulfonate group. After the sputtering, the carbon and sulfur become overpopulated at the surface. Therefore, the S/N ratio was considered to be useless in the depth analysis of the polyelectrolyte multilayer. Despite that, the Br/N ratio would provide some information; at least the data are comparable between the multilayers studied. The depth analysis reveals that there are small amounts of bromine just below the surface of the multilayer deposited in NaBrO₃ as can be seen in the Figure 4. The amount of bromine decreases sharply upon sputtering. The absence of bromine in the surface would indicate the easily exchangeable or removable nature of bromate ion. The depth analysis of the multilayer deposited in NaBr

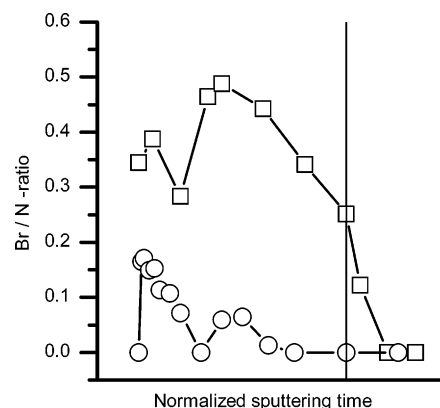


Figure 4. Sequential sputtering and XPS analysis of the PDADAMA/PSS multilayer. Multilayers are deposited in NaBrO₃ (circles) and NaBr (squares). Vertical line represents the raise of signal of gold, indicating that the film is sputtered thin enough for XPS to detect gold substrate. The sputtering times needed for the breakthrough are 40 and 240 min for the multilayer films deposited in NaBrO₃ and NaBr, respectively.

shows the presence of bromine both on the surface and in the bulk of film, with the Br/N ratio ranging from 1:3 to 1:2.

On the basis of the XPS measurements, the breakpoint in the Figure 3 can be attributed to a change in the charge compensation type. By using ClO₃⁻, NO₃⁻, or Br⁻ as the counteranion, the polymer charge density will be large enough to maintain the polymer solubility, but the deposited multilayer will most probably contain partly extrinsically compensated polymer. This polymer material would be stable because the ionic strength is kept constant during the measurement. For that reason, the PDADMA layers, formed in the presence of the above-mentioned counteranions and containing extrinsically compensated hydrophobic material, are not only deposited in considerably higher amounts but are relatively stiffer and develop plastic-like material together with rather hydrophobic PSS.

The stiffness of bulk multilayer is considerably higher than the stiffness of very thin water-swollen multilayers,¹⁶ in which the elastic properties are comparable to soft protein films.¹⁵ For that reason the elastic parameters obtained for very thin multilayers should not be regarded as representing the bulk material, as proven by the thick film measurements. The same observable fact can be also understood on the basis of the multilayer zone model. On the basis of our experience the hard core of the polyelectrolyte multilayer in the PDADMA–PSS system is present when approximately 20 layers of polyelectrolytes are deposited in the used concentration scale.

The comparison between the values of shear modulus measured by using QCM and the literature data must be done with caution. If we assume that the material follows the simple Voigt viscoelastic model with a single relaxation time as proposed by Höök et al.,¹⁵ we might compare the dynamic storage shear modulus with the static shear modulus and static elasticity modulus (Young's modulus). The dependence between Young's modulus (E) and shear modulus (G) for an elastomer is roughly the following: $G = E/3$. The shear modulus obtained from the polyelectrolyte microcapsules prepared from PDADMA and PSS is reported to be 140 MPa.⁹ The value is very close to the storage shear modulus obtained in our method if NaClO₃, NaNO₃, or NaBr is used in the deposition process. However, we

could not deposit a multilayer as stiff as that by using NaCl. The difference might be explained by the ionic strength effect, since the microcapsules were prepared in 0.5 M NaCl.⁹ The increasing ionic strength induces charge screening of a polyelectrolyte and would presumably lead into stiffening of the film. On the other hand, that is just a hypothesis, and it is not experimentally proven in this study. The high shear modulus value of the multilayer deposited in NaClO₃, NaNO₃, or NaBr could be realized as an offshoot when a polyelectrolyte multilayer was deposited inside the walls of outlet tubing of the measurement cell. Once dried, the free-standing very thin polyelectrolyte tubing could be detached and pulled out in one piece, hence showing a considerable tensile strength.

Because of the common use of sodium chloride in the studies of polyelectrolytes, special attention was paid to the multilayer deposition using NaCl. After five attempts we could not deposit more than 130 layers. Usually the complex LAI graph did not follow a smooth curve but had a random bend before 50 layers were completed. It would qualitatively indicate that the properties of the film change unexpectedly during the deposition process. We could think of no other explanation to this phenomenon than the breakpoint of material properties, which is located near the value of hydration entropy of chloride. The greater experimental error in the film parameters is explained by the smaller number of layers. It is unfortunate that chloride has been generally chosen as the most commonly used anion in the polyelectrolyte studies.

Conclusions

We have studied the deposition of PSS/PDADMA multilayers, containing a large number of layers, in the presence of different counteranions. The counteranion was found to affect not only by altering the mass but also the stiffness of the multilayer in a very significant manner. The storage shear modulus values varied between 6 and 130 MPa and bilayer mass density from 0.5 to 5 μg cm⁻². The increase of stiffness from fluoride to bromide is actually so great that it is comparable to the glass transition of common polymers. A correlation was found between the multilayer stiffness and the hydration entropy of corresponding counteranion, and a sharp breakpoint of material properties was found to be located near the hydration entropy value of chloride. The magnitude of increase at the breakpoint is actually so large that it would most probably involve structural changes in the multilayer. The increase in stiffness is probably due to the increased polyelectrolyte charge screening, and it is eventually, by using ClO₃⁻, NO₃⁻, or Br⁻ as a counteranion, leading to a situation where the polyelectrolyte charges are compensated partly by counterions in the polyelectrolyte multilayer. The deviation from the 1:1 polyelectrolyte complexes by the presence of small counteranions was also detected with XPS.

References and Notes

- (1) Decher, G. *Science* **1997**, *277*, 1232–1237.
- (2) Lvov, Y. M.; Decher, G.; Sukhorukov, G. *Macromolecules* **1993**, *26*, 5396–5399.
- (3) Kotov, N. A.; Dekany, I.; Fendler, J. H. *J. Phys. Chem.* **1995**, *99*, 13065–13069.
- (4) Lösche, M.; Schmitt, J.; Decher, G.; Bouwman, W. G.; Kjaer, K. *Macromolecules* **1998**, *31*, 8893–8906.
- (5) Dubas, S. T.; Schlenoff, J. B. *Macromolecules* **1999**, *32*, 8153–8160.
- (6) Mermut, O.; Barrett, C. J. *J. Phys. Chem. B* **2003**, *107*, 2525–2530.
- (7) Salomäki, M.; Tervasmäki, P.; Areva, S.; Kankare, J. *Langmuir* **2004**, *20*, 3679–3683.
- (8) Gao, G.; Donath, E.; Moya, S.; Dudnik, V.; Möhwald, H. *Eur. Phys. J. E* **2001**, *5*, 21–27.
- (9) Gao, C.; Leporatti, S.; Moya, S.; Donath, E.; Möhwald, H. *Langmuir* **2001**, *17*, 3491–3495.
- (10) Lulevich, V. V.; Radtchenko, I. L.; Sukhorukov, G. B.; Vinogradova, O. I. *J. Phys. Chem. B* **2003**, *107*, 2735–2740.
- (11) Lulevich, V. V.; Radtchenko, I. L.; Sukhorukov, G. B.; Vinogradova, O. I. *Macromolecules* **2003**, *36*, 2832–2837.
- (12) Mermut, O.; Lefebvre, J.; Gray, D. G.; Barrett, J. *Macromolecules* **2003**, *36*, 8819–8824.
- (13) Picart, C.; Sengupta, K.; Schilling, J.; Maurstad, G.; Ladam, G.; Bausch, A. R.; Sackmann, E. *J. Phys. Chem. B* **2004**, *108*, 7196–7205.
- (14) Lucklum, R.; Behling, C.; Cernosek, R. W.; Martin, S. J. *J. Phys. D: Appl. Phys.* **1997**, *30*, 346–356.
- (15) Höök, F.; Kasemo, B.; Nylander, T.; Fant, C.; Sott, K.; Elwing, H. *Anal. Chem.* **2001**, *73*, 5796–5804.
- (16) Lukkari, J.; Salomäki, M.; Ääritalo, T.; Loikas, K.; Laiho, T.; Kankare, J. *Langmuir* **2002**, *18*, 8496–8502.
- (17) Lee, S.-W.; Hinsberg, W. D.; Kanazawa, K. K. *Anal. Chem.* **2002**, *74*, 125–131.
- (18) Wägberg, L.; Pettersson, G.; Notley, S. *J. Colloid Interface Sci.* **2004**, *274*, 480–488.
- (19) Salomäki, M.; Loikas, K.; Kankare, J. *Anal. Chem.* **2003**, *75*, 5895–5904.
- (20) Ladam, G.; Schaad, P.; Voegel, J. C.; Schaaf, P.; Decher, G.; Cuisinier, F. *Langmuir* **2000**, *16*, 1249–1255.
- (21) Hickman, J. J.; Laibinis, P. E.; Auerbach, D. I.; Zou, C.; Gardner, T. J.; Whitesides, G. M.; Wrighton, M. S. *Langmuir* **1992**, *8*, 357–359.
- (22) Kankare, J.; Loikas, K. Patent pending.
- (23) Kankare, J. *Langmuir* **2002**, *18*, 7092–7094.
- (24) Marcus, Y. *Ion Solvation*; Wiley: Chichester, 1985.
- (25) Caruso, F.; Niikura, K.; Furlong, D. L.; Okahata, Y. *Langmuir* **1997**, *13*, 3422–3426.
- (26) Baba, A.; Kaneko, F.; Advincula, R. C. *Colloids Surf., A* **2000**, *173*, 39–49.
- (27) Du, B.; Johannsmann, D. *Langmuir* **2004**, *20*, 2809–2812.
- (28) Aklonis, J. J.; MacKnight, W. J. *Introduction to Polymer Viscoelasticity*, 2nd ed.; John Wiley and Sons: New York, 1983.
- (29) Jones, G.; Dole, M. *J. Am. Chem. Soc.* **1929**, *51*, 2950–2964.
- (30) Jenkins, H. D.; Marcus, Y. *Chem. Rev.* **1995**, *95*, 2695–2724.
- (31) Hofmeister, F. *Arch. Exp. Pathol. Pharmacol.* **1888**, *24*, 247–260.
- (32) Schlenoff, J. B.; Ly, H.; Li, M. *J. Am. Chem. Soc.* **1998**, *120*, 7626–7634.
- (33) Yoo, D.; Shiatori, S. S.; Rubner, M. F. *Macromolecules* **1998**, *31*, 4309–4318.
- (34) Shiatori, S. S.; Rubner, M. F. *Macromolecules* **2000**, *33*, 4213–4219.
- (35) Schlenoff, J.; Ly, H.; Li, M. *J. Am. Chem. Soc.* **1998**, *120*, 7626–7634.
- (36) Büscher, K.; Graf, K.; Ahrens, H.; Helm, C. A. *Langmuir* **2002**, *18*, 3585–3591.
- (37) Xie, A. F.; Granick, S. *Macromolecules* **2002**, *35*, 1805–1813.
- (38) Caruso, F.; Lichtenfeld, H.; Donath, E.; Möhwald, H. *Macromolecules* **1999**, *32*, 2317–2328.
- (39) Laurent, D.; Schlenoff, J. *Langmuir* **1997**, *13*, 1552–1557.
- (40) Takahagi, T.; Ishitani, A. *Macromolecules* **1987**, *20*, 404–407.